Chemistry, Biology, and Physical Sciences Academic Journal
Vol.07, Issue 4; October–December, 2025;
ISSN (3773–5391);
p –ISSN 7122–5392;
Impact factor: 6.53

COLOCASIA-ESCULENTA-MEDIATED SYNTHESIS OF ZINC OXIDE NANOPARTICLES FOR ANTIMICROBIAL APPLICATIONS

T. P Ugosor[*] and T.T Ornguga[1]
[*]Department of Chemistry, College of Education, Katsina-Ala, Benue State, Nigeria.
T.P Ugoosor ORCID ID: https://orcid.org/0009-0001-1815-5057
[1]Department of Biology, College of Education, Katsina-Ala, Benue State, Nigeria.
T.T Ornguga ORCID ID: https ://orcid.org/0009-0001-8255-7376
Corresponding author: paulugosor@gmail.com, 08032980396

Abstract: Zinc oxide nanoparticles (ZnO NPs) were successfully synthesized using an eco-friendly green approach mediated by the aqueous leaf extract of *Colocasia esculenta*. The nanoparticles were characterized through UV–Visible spectroscopy, X-ray diffraction (XRD), scanning electron microscopy (SEM), energy-dispersive X-ray spectroscopy (EDX), and Fourier-transform infrared spectroscopy (FTIR). The antimicrobial potential of the biosynthesized ZnO NPs was evaluated against selected fungal and bacterial pathogens. XRD revealed a wurtzite hexagonal ZnO structure with an average crystallite size of 17.56 nm. FTIR spectra indicated phenolics, amines, and amides as capping and stabilizing agents. The antimicrobial efficacy of the ZnO NPs was tested against selected fungi: *Aspergullus tamari, Penicillium marneffei, Rhizopus stolenifera, Fussarrium solani and Rhizopus nigrican* and *bacteria: Escherichia coli, Erwinia carotovora, and Pseudomonas aeruginosa*. The ZnO NPs exhibited significant antimicrobial activity, showing inhibition from 43.33 % (moderate) to 85.54 % (effective). These findings highlight the potential of ZnO NPs as cost-effective, eco-friendly alternatives for antimicrobial formulation.

Keywords: *Colocasia esculenta*, Zinc oxide nanoparticles, Green synthesis, Phytochemicals, Antimicrobial activity, Pathogens

1.0 Introduction

The accelerating global burden of multidrug-resistant (MDR) bacteria and fungi is undermining decades of advances in anti-infective therapy and elevating morbidity, mortality, and health-care costs worldwide. Recent global estimates predict a dramatic rise in deaths attributable to antibiotic-resistant infections unless effective interventions are deployed, with the greatest impact expected in low- and middle-income regions that already experience high infectious-disease burdens [1, 2, 3]. These projections, together with repeated reports of treatment failures for common pathogens (e.g., *Escherichia coli, Staphylococcus aureus, Pseudomonas aeruginosa,* and *carbapenem*-resistant *Enterobacterales, Candida* spp, *Erwinia corotovora,* etc), highlight the urgent need for novel, affordable, and environmentally sustainable antimicrobial approaches.

Nanotechnology provides one such avenue by enabling the design and application of functional nanomaterials that act via multimodal mechanisms less susceptible to classical resistance pathways [4, 5]. Among metal-oxide nanomaterials, zinc oxide nanoparticles (ZnO-NPs) combine favourable physicochemical properties: biocompatibility, chemical stability, and strong antimicrobial activity with relatively low production cost compared with noble-metal nanoparticles. ZnO-NPs exert antimicrobial effects through several complementary mechanisms, including generation of reactive oxygen species (ROS), release of Zn^{2+} ions that disturb metal homeostasis, and direct disruption of microbial membranes and metabolic processes [6, 7, 8]. These multifaceted actions reduce the probability that single-step genetic mutations will confer high-level resistance, making ZnO-NPs particularly attractive as alternatives or adjuvants to conventional antibiotics [9, 10].

However, many conventional physicochemical routes for ZnO-NPs production (sol–gel, hydrothermal, chemical vapour deposition) require hazardous reagents, high temperatures, or complex

Chemistry, Biology, and Physical Sciences Academic Journal
Vol.07, Issue 4; October–December, 2025;
ISSN (3773–5391);
p –ISSN 7122–5392;
Impact factor: 6.53

instrumentation that elevates cost and environmental footprint, factors that constrain large-scale deployment, particularly in resource-limited settings. To address these limitations, "green" or biological synthesis methods have been developed that exploit plant extracts, microbial metabolites, or biopolymers as reducing and capping agents. Plant-mediated (phytosynthesis) approaches are especially appealing: plant biomolecules (phenolics, flavonoids, terpenoids, proteins, alkaloids, glycosides etc) simultaneously reduce zinc precursors and stabilize nanoparticles under mild conditions, thus minimizing toxic by-products and energy input while often improving biological compatibility [8, 11, 12]. Numerous recent reviews and empirical studies report that green-synthesized ZnO-NPs possess comparable or superior antimicrobial potency to chemically synthesized analogues, with easier scalability and lower environmental risk [13, 14].

Empirical evidence for the antimicrobial efficacy of green ZnO-NPs is rapidly accumulating. Studies using a variety of plant extracts have demonstrated strong *in vitro* activity against Gram-positive and Gram-negative bacteria, as well as yeasts and filamentous fungi; reported minimum inhibitory concentrations (MICs) and inhibition-zone diameters indicate dose-dependent bactericidal and fungicidal effects in many strains, including clinically relevant MDR isolates [15, 16]. In several reports, plant-derived ZnO-NPs also inhibited biofilm formation and disrupted established biofilms, an important advantage because biofilms are major drivers of chronic infection and antibiotic tolerance [17]. Collectively, these data suggest that green ZnO-NPs could be deployed in topical formulations, coatings, or as adjuncts to antibiotic therapy to reduce microbial load, prevent surface contamination, and limit selection for resistant clones [18]. Economics and sustainability are central to the translation of any new antimicrobial technology. Green synthesis using widely available plant materials (e.g., agricultural by-products or fast-growing medicinal plants) reduces both raw-material costs and dependence on toxic reagents, while simple processing enables decentralised production in low-resource settings. This decentralized, low-energy model better aligns with One Health goals and with the urgent need to provide cost-effective interventions in regions experiencing acute AMR burdens, such as sub-Saharan Africa. Country-level AMR assessments highlight high prevalence and diverse drivers of resistance (over-the-counter antibiotic sales, weak diagnostics and stewardship, agricultural antibiotic use), emphasizing that locally appropriate, affordable antimicrobial technologies are urgently required.

Despite these advantages, several scientific and regulatory gaps must be addressed before green ZnO-NPs can be widely recommended. Key research priorities include:

(i) Standardization of synthesis protocols to ensure reproducible particle size, morphology, and surface chemistry, parameters that directly influence antimicrobial potency and toxicity;

(ii) Rigorous cytotoxicity and ecotoxicity assessment across relevant mammalian cell types and environmental compartments;

(iii) Mechanistic studies against MDR clinical isolates and biofilms, including synergy testing with existing antibiotics; and

(iv) Scalable manufacturing models and regulatory pathways for medical and environmental applications.

Addressing these gaps will require multidisciplinary collaboration: combining materials science, microorganism hazards, toxicology, and public-health policy to translate laboratory promise into safe, effective, and equitable solutions.

In this context, the present work investigates plant-mediated ZnO nanoparticle synthesis using *Colocasia esculenta* leaves extract, performs detailed physicochemical characterization (UV-Vis, XRD, SEM-EDX, FT-IR), and evaluates antibacterial and antifungal activity against a panel of clinically relevant MDR strains of microorganisms. We hypothesize that green-synthesized ZnO-NPs offer a pragmatic, eco-friendly, and cost-effective strategy to mitigate MDR infections, particularly as topical agents, disinfectants, or antibiotic adjuvants, provided that synthesis and safety parameters are standardized and that application-specific toxicological data corroborate efficacy.

2.0 Materials and Methods

2.1 Material

Fresh leaves of *Colocasia esculenta* were collected, authenticated, air-dried, and powdered. Previously isolated pathogens, including five fungi: *Aspergullus tamari, Penicillium marneffei, Rhizopus stolenifera, Fussarrium solani and Rhizopus nigrican* and *three bacteria: Escherichia coli, Erwinia carotovora*, and

Chemistry, Biology, and Physical Sciences Academic Journal
Vol.07, Issue 4; October–December, 2025;
ISSN (3773–5391);
p –ISSN 7122–5392;
Impact factor: 6.53

Pseudomonas aeruginosa were obtained from the Biological Science laboratory of Rev. Fr. Moses Orshio Adasu University, Makurdi, Benue State.

The culture media: Nutrient broth, Potato Dextrose Agar (PDA), Nutrient Agar (NA), Simon citrate Agar, Triple Sugar Iron Agar (TSIA), and MacConkey Agar were sourced from, TITAN BIOTECH TM MEDIA, RAJASTHAN, INDIA through Agbe Science, Makurdi, Benue State, Nigeria. Grams staining reagents (Luggol`s iodine, crystal violet, safranin, and absolute ethanol); catalase reagent (hydrogen peroxide); oxidase; Covacs reagents; ethanol, methanol, methylated spirits and sodium hypochlorite were also sourced from BDH Chemicals, England, M&B laboratory, England and Agbe Science, Makurdi, Benue State, Nigeria. Zinc acetate was sourced from CHEMETAL (Malaysia) Sdn. Bhd through Emole (Nig) LTD, Makurdi, Benue State, Nigeria.

All reagents were of analytical grade and were used without any additional purification. Fresh solutions were prepared with double-distilled water and stored in dark conditions to minimize photochemical degradation of sensitive compounds. Prior to use, all glassware was sterilized by immersion in 10% sodium hypochlorite solution, thoroughly rinsed with double-distilled water, and air-dried. All experimental procedures were conducted under aseptic conditions to prevent contamination.

2.2 Methods

Standard analytical methods of the Official Methods of Analytical Chemists, AOAC, (2023) [19] were employed to extract the *Colocasia esulenta* leaves and carryout phytochemical analysis, while microbial studies were performed by methods of Clinical and Laboratory Standards Institute CLSI, (2024) [20].

ZnO NPs was synthesized and characterized by methods described by [4, 7] using UV-Vis, XRD, SEM-EDX, and FTIR techniques.

Antimicrobial testing was conducted using agar well diffusion [20], and data were analyzed using ANOVA and DMRT at $p < 0.05$.

2.2.1 Drying and pulverization of *Colocasia esculenta* leaves

Colocasia esculenta leaves were carefully washed with distilled water and dried afterwards under a shade at room temperature to avoid chemical decomposition for two weeks. After drying, the leaves were ground into fine powder using a wooden mortar and pestle. The powdered material was kept in a plastic jar with air tight lid.

2.2.2 Plant extraction procedure

The extract was prepared by adding 200 g of powdered material to 1000 mL of distilled water. The mixture was heated at 80°C for 30 minutes, allowed to cool in a desiccator, and then filtered to obtain the extract.

2.2.3 Storage of the extract

Extractwas refrigerated at 4 ^{o}C for further analysis.

2.3.4 Culture media preparation

The methods of Clinical and Laboratory Standards Institute performance standards (CSLI) for antimicrobial sensitivity test, 2024) were used without modifications.

2.4 Qualitative phytochemical analysis

Preliminary qualitative phytochemicals analysis was performed using standard analytical procedures as described by Oluwatosin et al., (2020) [21] without any modification.

2.5 Antimicrobial Sensitivity Test

The method of Terngu et al., (2024) [7] was employed without modifications. The NPs was tested against five pathogenic fungi: *Aspergullus tamari*, *Penicillium marneffei, Rhizopus stolenifera, Fussarrium solani and Rhizopus nigrican* and *bacteria: Escherichia coli, Erwinia carotovora,* and *Pseudomonas aeruginosa*.

Zone of inhibition (mm) where present was recorded with a transparent plastic ruler after the incubation period and the percentage inhibition zones calculated as shown below:

$$\% \text{ Inhibition Zone (\% IZ)} = \frac{\text{Average diametre of pathogen colony}}{\text{Average diametre of pathogen in control}} \times 100\ \%.$$

The percentage inhibition was rated on the scale described by Terngu et al., (2024) as follows:

100 % inhibition (highly effective); 50 – 99 % inhibition (effective); 20 – 49 % inhibition (moderately effective); 0 – 19 % inhibition (slightly effective) and ≤ 0 % inhibition (not effective).

3.0 Results and Discussion

3.1 Phytochemical Screening

The preliminary phytochemical analysis result of the aqueous leaves extract of *Colocasia esculenta* is presented in Table 1. The result revealed the presence of saponins, alkaloids, flavonoids, glycosides, terpenoids, polyphenols, tannins, steroids and starch as

Chemistry, Biology, and Physical Sciences Academic Journal
Vol.07, Issue 4; October–December, 2025;
ISSN (3773–5391);
p –ISSN 7122–5392;
Impact factor: 6.53

bioactive compounds serving as reducing and stabilizing agents.

Table 1: Result of phytochemical screening

Secondary Metabolite	Test	Result
Saponnins	Foam Test	+
Alkaloids	Hager's Test	+
Flavonoids	Shinoda Test	+
Glycosides	Salkowski's Test	+
Terpenoids	Chloroform Test	+
Polyphenols	Ferric chloride Test	+
Tannins	Ferric chloride Test	+
Steroids	Libermann-Burchard's test	+
Starch	Iodine Test	+
Quinones	Hydrochloric acid test	-

Key: + = Presence of secondary metabolite; - = Absence of secondary metabolite.

3.2 Characterization of ZnO NPs

3.2.1 UV-Visible Spectroscopy Analysis

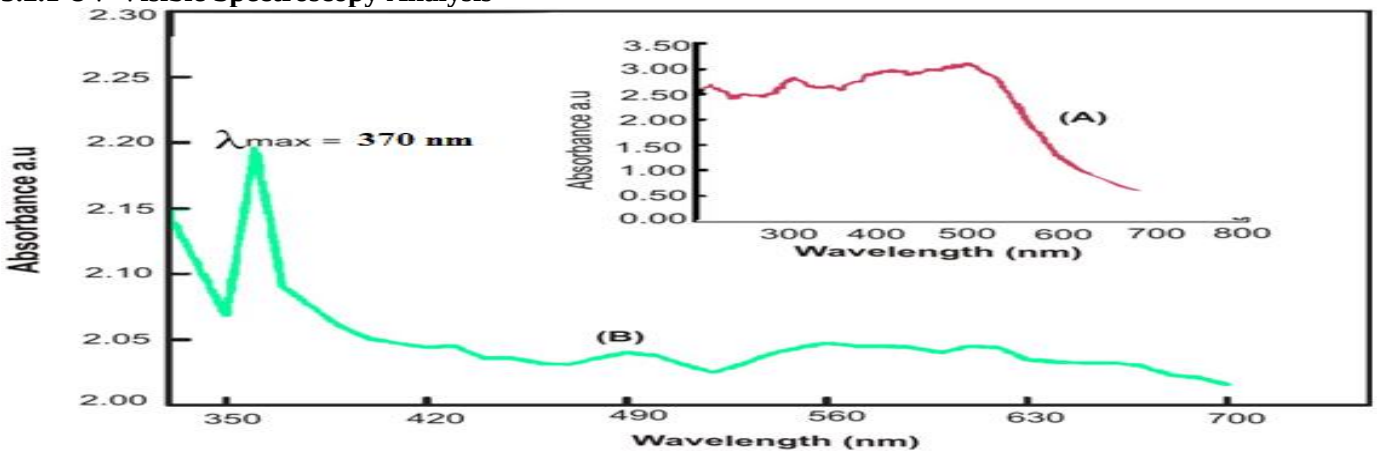

Figure 1: UV-Visible spectra of (A) *Colocasia esculenta* leaves extract and (B) Zno NPs.

UV-visible spectrophotometry is an efficient, reliable and cost-effective analytical method that is used for the confirmation of the formation of nanoparticles. This technique is widely used for the structural characterization of nanoparticles. UV–Vis spectroscopy showed an absorption peak at 370 nm, confirming nanoparticle formation. SPR peak at 370 nm, which verifies synthesis of the nanoparticles, was created by the reaction of light with the surface electrons of ZnO/*C. esculenta* extract.

The tuber peel extract from *C. esculenta* showed intense peaks at 321 nm, 284 nm, and 214 nm. These peaks are caused by the phytochemicals in the extract (Figure 1A). *Colocasia esculenta* is known to contain phytochemicals like saponnins, tannins, phenolic compounds, steroids, alkaloids, glycosides as well as terpenes like neoxanthin and lutein, which serve as redcutants, capping and stabilization of nanoparticles (17).

3.2.2 XRD Analysis

Chemistry, Biology, and Physical Sciences Academic Journal
Vol.07, Issue 4; October–December, 2025;
ISSN (3773–5391);
p –ISSN 7122–5392;
Impact factor: 6.53

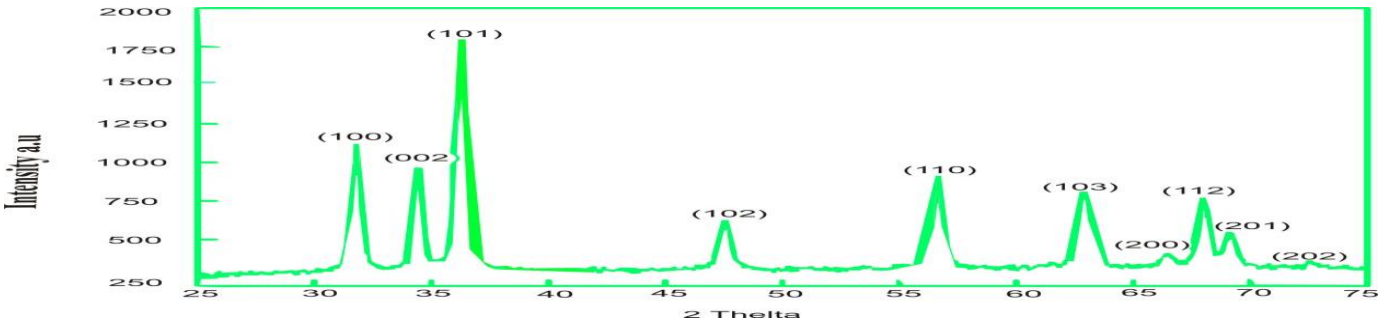

Figure 2: XRD patterns of ZnO NPs

As a quick, flexible, and non-destructive analytical technique, X-ray diffraction can be used to identify and quantify different crystalline forms, or "phases," as well as unit cell diameters and the purity of powdered or solid materials. The interaction of the incident rays in a diffractometer with the sample produces diffracted rays when conditions satisfy Bragg`s law
$(n\lambda) = 2d\sin\theta$, where n = 1, 2, 3, θ = diffraction angle, d = interplaner spacing, and λ = X-ray wavelength [17]. Ten distinct peaks at 2θ of 32.02°, 34.48°, 36.85°, 47.59°, 56.65°, 62.98°, 66.96°, 67.14°, 68.12°, and 72.95° were seen in the XRD spectra of the ZnO NPs. These peaks corresponds to the hexagonal closed pack (HCP) ZnO NPs' (100), (002), (101), (102), (110), (103), (112), (200), (201), and (202) reflection lines when compared with the Joint Committee on Powder Diffraction Standards (JCPDS) database number 00-004-0784 [4, 5]. The clearly defined, intense and sharp peaks in the XRD pattern of the nanoparticles showed that the particles portray high degree of crystalinity [4]. The XRD spectra thus shows that the biosynthesized ZnO nanoparticles are crystalline [18].

XRD analysis confirmed a wurtzite hexagonal ZnO structure with an average crystallite size of 17.56 nm.

3.2.3 SEM-EDX Analysis

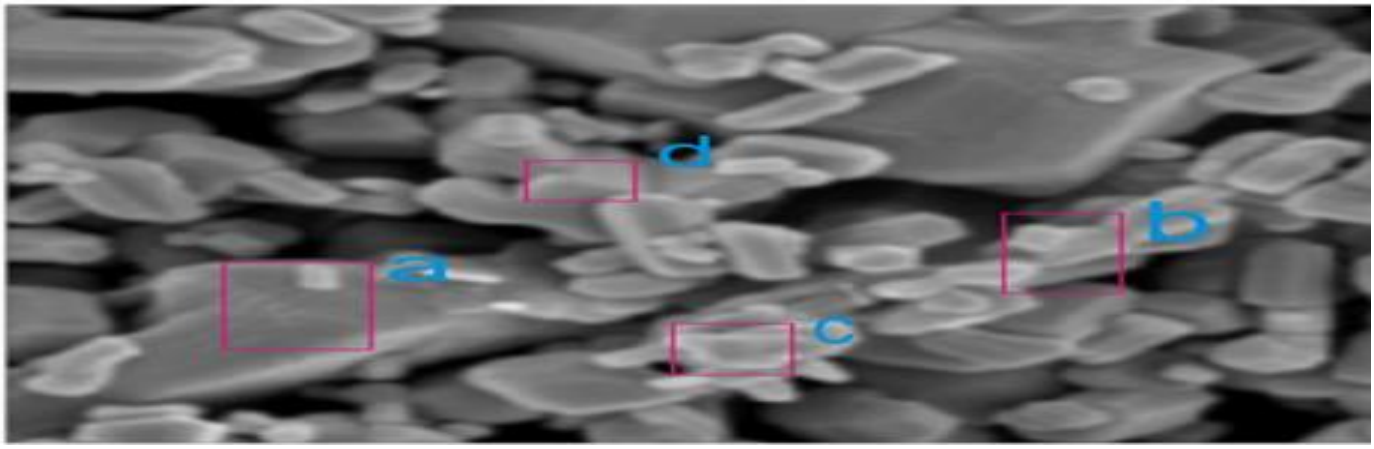

Figure 3: SEM images of ZnO NPs.

Surface morphology, sizes and crystallites distribution of the zinc oxide nanoparticles were examined with the aid of scanning electron microscopy with spectral imaging system and equipped with EDX. SEM and EDX analyses indicated uniform hexagonal wurtzite morphology with high Zn and O purity with average crystallite size of 17.60 nm. The locations of the measurements are denoted by a, b, c, and d. The ZnO NPs' SEM micrographs revealed slightly agglomerated/aggregated nanoparticles, most likely as a result of biological molecules adhering to one another, smaller crystallite sizes, nanoparticle interaction, or ageing effects brought on by refluxing conditions [4, 9]. This result correlates with that of the XRD analysis.

3.2.4 EDX Analysis

Chemistry, Biology, and Physical Sciences Academic Journal
Vol.07, Issue 4; October–December, 2025;
ISSN (3773–5391);
p –ISSN 7122–5392;
Impact factor: 6.53

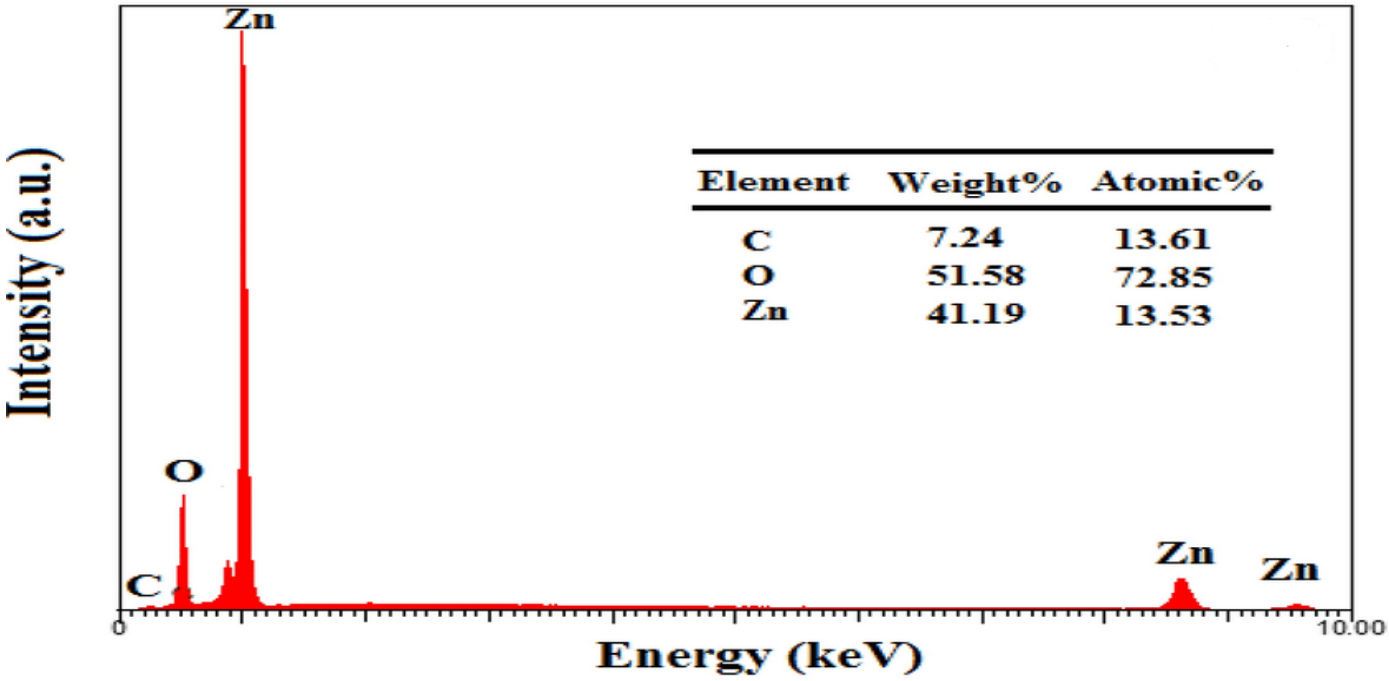

Figure 4: EDX Spectra of ZnO NPs.

EDX spectrum shows three prominent peaks (peak maxima) that are directly associated with the zinc content of the sample. As shown by XRD spectra, the reaction products are made up of high purity ZnO nanoparticles as a result of the high percentage of Zn and O, but low percentage of C. The intense peaks suggest that Zn and O are the major elements in the ZnO NPs.

3.3.5 FTIR Analysis

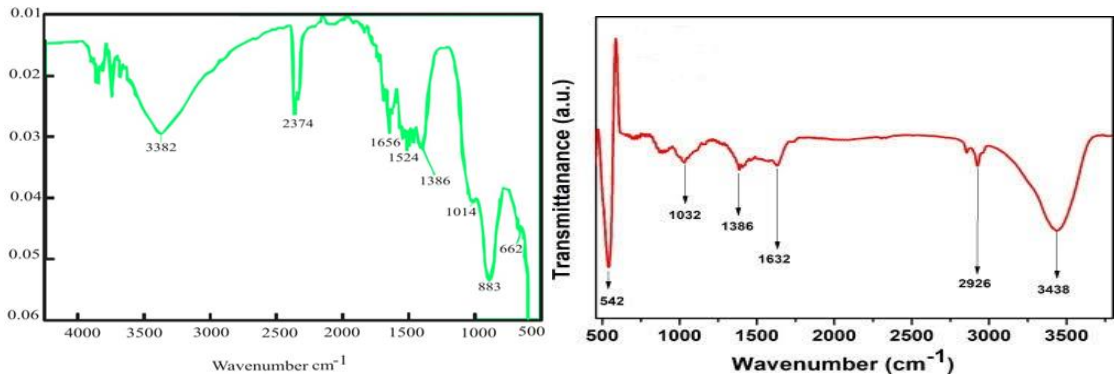

(A) **(B)**

Figure 5: FTIR spectra of (A) *Colocasia esculenta* Leaves extract and (B) ZnO NPs

Fourier transform infrared spectroscopy (FTIR) is a sophisticated and widely used analytical technique for determining chemical structures or functional groups of infrared-active substances [11]. FTIR spectra identified functional groups responsible for nanoparticle formation. Figure 5 displays the FTIR absorption spectra of the *Colocasia esculenta* extract and ZnO NPs. The spectra illustrate the production of distinctive transmission peaks the extract at around 3281 cm^{-1}, 2918 cm^{-1}, 2831 cm^{-1}, 1734 cm^{-1}, 1596 cm^{-1}, 1410 cm^{-1}, 1370 cm^{-1}, 1232 cm^{-1}, 1022 cm^{-1}, and 532 $cm^{-1,}$ respectively. The peakat 2918 cm^{-1} shows creatine, cholesterol, and phospholipids. Peak 3281 cm^{-1} shows symmetric O-H stretching, possibly from phenolics

Chemistry, Biology, and Physical Sciences Academic Journal
Vol.07, Issue 4; October–December, 2025;
ISSN (3773–5391);
p –ISSN 7122–5392;
Impact factor: 6.53

[16]. The C-H and C=O stretching of alkanals/aldehydes, alkanones/ketones, and esters/alkanoates are attributed to the peaks at 2831 cm^{-1} and 1734 cm^{-1} [12]. C-N and NH_2 adenine are represented by the peaks at 1596 cm^{-1}; C-N stretching and N-H deformations are allocated to 1410 cm^{-1}, and N-H and C-H deformations are assigned to 1370 cm^{-1}. The peak 1232 cm^{-1}, reveals overlapping of the protein amide III and nucleic acid phosphate vibrations. Peaks 1022 cm^{-1}, and 532 cm^{-1}represent glycogen, and sulphur compounds respectively [12, 16].

The Zn-O bond (ZnO wurtzite hexagonal phase) is characterized by the FTIR spectrum's extremely small peak at 542 cm^{-1} as a result of Zn-O vibrations of ZnO nanoparticles [13]. The smaller crystallite sizes may be explained by the increased absorption caused by the low precursor concentration [13, 14, 15]. According to the results of other studies, smaller crystallite sizes are associated with greater shifts in absorbance and band area (Mohhamed & Shafey, 2020; Abdullah et al., 2020; 2022; Iayanchandran & Nair, 2022). These findings suggest that phenolic compounds perform a major function in the reduction of Zn^{2+} that occurs during synthesis [17, 22].

3.3 Antimicrobial Sensitivity Test

Table 2: Antimicrobial sensitivity test result: Average zone of inhibition (mm)

ZnO NPs Concentration (mg/mL)					
	100	**75**	**50**	**25**	**Control**
Fungi					
A. tamari	8.82 ± 0.01^a	7.90 ± 0.02^b	6.91± 0.01^c	5.01 ± 0.02^d	10.31± 0.02^e
P. marneffei	9.12 ± 0.01^a	8.95± 0.02^b	7.54±0.01^c	6.70 ± 0.01^d	13.15± 0.01^e
R. stolenifera	13.60 ± 0.01^a	11.16± 0.01^b	9.50± 0.01^c	7.80 ± 0.01^d	18.00 ± 0.01^e
F. solani	20.50 ± 0.02^a	18.33 ± 0.02^b	17.33 ± 0.01^c	15.93± 0.01^d	24.67 ± 0.02^e
R. nigrican	11.81 ± 0.02^a	10.10 ± 0.02^b	9.00 ± 0.03^c	8.14 ± 0.02^d	14.16± 0.02^e
Bacteria					
E. coli	40.28 ± 0.02^a	38.10 ± 0.02^b	35.89 ± 0.02^c	35.12 ± 0.01^d	50.12 ± 0.02^e
E. carotovora	52.24 ± 0.01^a	48.89 ± 0.01^b	45.13 ± 0.02^c	42.98 ± 0.02^d	63.19 ± 0.01^e
P. aeruginosa	37.26 ± 0.02^a	34.89 ± 0.02^b	31.93 ± 0.01^c	28.38 ± 0.01^d	45.67± 0.01^e

N=5: Means followed by different alphabetical letters (superscript) within the same row are significantly different ($p < 0.05$) according to ANOVA and Duncan's Multiple Range Test (DMRT).

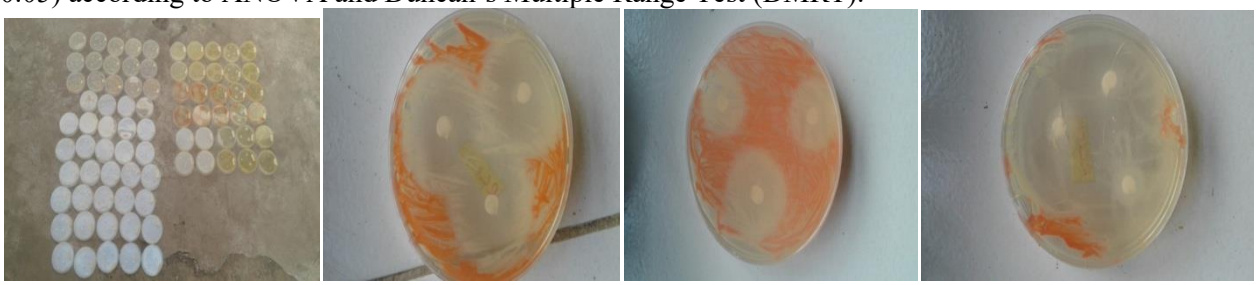

Figure 6: Antimicrobial sensitivity test plates

Table 3: Percentage zone of inhibition of ZnO NPs

Concentration (mg/mL)	100	75	50	25
Fungi				
Aspergillus tamari	85.54	76.62	67.02	48.59
Penicillium marneffei	69.35	68.06	57.34	50.95
Rhizopus stolenifera	75.56	62.00	52.78	43.33
Fussarrium solani	83.10	74.30	70.25	64.57

Chemistry, Biology, and Physical Sciences Academic Journal
Vol.07, Issue 4; October–December, 2025;
ISSN (3773–5391);
p –ISSN 7122–5392;
Impact factor: 6.53

Rhizopus nigrican	83.40	71.33	63.56	54.49
Bacteria				
Escherichia coli	80.37	76.02	71.61	70.07
Erwinia carotovora	82.67	77.40	71.42	68.02
Pseudomonas aeruginosa	81.59	76.40	69.91	62.14

Key:
a = 100 % inhibition (highly effective)
b = 50 – 99 % inhibition (effective)
c = 20 – 49 % inhibition (moderately effective)
d = 0 -19 % inhibition (slightly effective)
e = ≤ 0 % inhibition (not effective) (Terngu et al., 2024).

Table 2 represents average zone of inhibition while Table 3 shows the percentage inhibition zone of the ZnO NPs. The ZnO NPs demonstrated concentration-dependent antimicrobial activity, showing inhibition zones up to 85.54 % against *Aspergillus tamari* and 43.33 % against *Rhizopus stolenifera* at 100 mg/mL and 25 mg/mL respectively. These results affirm that ZnO NPs synthesized via *Colocasia esculenta* extracts are effective, eco-friendly antimicrobial agents suitable for the management of multi-drug resistant strains of microorganisms.

4.0 Conclusion

The green synthesis of ZnO NPs using *Colocasia esculenta leaf* extract yielded highly pure, hexagonal nanoparticles with strong antimicrobial activity. Their performance against both fungal and bacterial pathogens was comparable to standard antibiotics: Voriconazole (fungi) and Gatifloxacin (bacteria), demonstrating their potential as safe, sustainable alternatives for management of multi-drug resistant strains and antimicrobial formulations.

Acknowledgement

The authors acknowledge the Departments of Chemistry and Biological Sciences, College of Education, Katsina-Ala for providing laboratory support during this study.

Conflict of Interest

The authors declare no conflict of interest.

References

World Health Organization. (2025). Global Antimicrobial Resistance and Use Surveillance System (GLASS) report: antibiotic use data for 2022. World Health Organization.

World Health Organization. (2023, November 21). Antimicrobial resistance—fact sheet. World Health Organization.

Centers for Disease Control and Prevention. (2022). Antimicrobial resistance threats in the United States, 2019: Update 2022. U.S. Department of Health & Human Services, CDC.

Jayanta, K.B., &Dillip, K, B. (2023). Synthesis and Characterization of Zinc Oxide Nanoparricles. International Journal of Nanomedicine, 13:1603-1620.

Johar, A. A.A., Mercedes J, R., Antonio, G., & Alberto. R. (2022). Eco-friendly synthesis of ZnO-nanoparticles using Phoenix dactyliferaL. polyphenols: physicochemical, microstructural and functional assessment. Res earch Square. https://orcid.org/0000-0002-5923-8254.

Ahmed, S.A., Taia, A., Ahmad, O.B., Samy, S., Abir, M.H. (2022). A.Green Synthesis and Characterization of ZnO Nanoparticles Using Pelargonium odoratissimum(L.) Aqueous Leaf Extract and Their Antioxidant, Antibacterial and Anti-inflammatory Activities. Antioxidants (Basel).2022;(8):1444.DOI:10.3390/antiox11081444.Available:https://doi.org/10.4236/fns.2017.87051.

Terngu, P.U., Anhwange, A., Okibe, F.G and Dooshima, S. (2024). Green synthesis of Zinc Oxide Naniparticles using Colocasiaesculenta Tuber Peel Extract and Antimicrobial Studies

Aganist White Yam Pathogens. Asian J. Food Res. & Nutri., vol. 3, no. 2, pp. 306- 319, 2024; Article no.AJFRN.116492.

Rahayu, V., Wonoputri, V, & Samadhi, T.W. (2020). Plant extract-assisted biosynthesis of zinc oxide nanoparticles and their antibacterial applications. Material Science and Engineering 823;012036.

Rajendran, N.K. George, B.P., Houreld , N.N., &Abrahamse, H. (2021). Synthesis of zinc oxide nanoparticles using Rubusfairholmianus root extract and their activity against pathogenic bacteria. molecules, 26, 1-11.

Rivero, K.T., Arrieta, J.B., Fiol, N, & Florido, A. (2021). Metal and metaloxide nanoparticles: Anintegrated perspective of the green synthesis methods by natural products and waste valorization:applicationsan dchallenges.Comprehensive AnalyticalChemistry,ed.S.K.VermaandA.K.Das ,Elsevier,94, ch. 10,433-469.

Sunday, A.A., & Aderonke, S. (2020). A Review of the Green Synthesis of Zinc Oxide Nanoparticles using Plant Extract.Bionanoscien ce.https://doi.org/10.1007//s12668 -020-00774- 6.

Xu, J., Huang, Y., Zhu, S., Abbes, N., Jing, X.,& Zhang, L. (2021). A review of the green synthesis of ZnO nanoparticles using plant extracts and their prospects for application in antibacterial textiles. Journal Engineering Fibers Fabrication, 16: 1-14.

Liu, Y. C., Li, J., Ahn, J., Pu, J., Rupa, E. J., Huo, Y.,& Yang, D. C. (2020). Biosynthesis of zinc oxide nanoparticles by one-pot green synthesis using fruit extract of Amomumlongigulare and its activity as a photocatalyst. Optik, 218: 165245.

Jin, S.,& Jin, H. (2021). Antimicrobial activity of zinc oxide nano/microparticles and their combinations against pathogenic microorganisms for biomedical applications: from physicochemical characteristics to pharmacological aspects. Nanomaterials (Basel, Switzerland), 11(2): 263

Jiang, S., Lin, K, & M. Cai, M. (2020). ZnOnanomaterials: current advancements in antibacterial mechanisms and applications. Front. Chem., 2020, **8**, 1-5.

Javed, R., Zia, M., Naz, S., Aisida, S. O., Ain, N. U. & Ao, Q. (2020). Role of capping agents in the application of nanoparticles in biomedicine and environmental remediation: recent trends and future prospects. Journal Nanobiotechnology, 18: 172

Farjana, R., Md Abdul M.P., Md Abu, B.S, Muhammad, S.B, Md. Aminul, H., Beauty, A., Rimi, R., Md. Anamul, H., Royhan, A.K.M. (2022). Green synthesis of ZnO nanoparticles using Cocos nucifera leaf extract: Characterization, antimicrobial, antioxidant, and photocatalytic activity; 2022. Available:https//doi.org/10.11012020.10.27.51 4023.

Priyatharesini, P.I., Ganesamoorthy, R., Sudha, R. (2020). Synthesis of zinc oxide nanoparticle using Cocosnuciferamale flower extract and analysis of their antimicrobial Activity. J of Pharm and Tech. 2020;13:2151- 2154.

Official Methods of Analysis of AOAC International. (2023). 22nd ed. AOAC International, Gathersburg, MD, USA, Official Methods, 2023.005

Clinical and Laboratory Standard Institute, CLSI.(2024). Performance Standards for Antimicrobial Susceptibility Testing.https://clsi.org/media/2481/m100edz0.s ample.

Oluwatosin, O. T., Adesina, J. M., & Ogunyemi, O. O. (2020). Phytochemical screening and antimicrobial properties of *Moringa oleifera*

leaf extract. Journal of Medicinal Plants Studies, 8(2), 77–82.

Eleazu, C.0. (2016). Characterization of the natural products in cocoyam (*Colocasia esculenta*) using GC-MS. Pharmaceutical Biology. 2016;54(12):2880-2885.